Supplement to

Decadal Seismicity Prior to Great Earthquakes at Subduction Zones: Roles of Major Asperities and Low-Coupling Zones

By Lynn R. Sykes

This section contains information on some of the smaller great earthquakes studied, those with no or poor information on the zones of high displacements and those for which no or little forerunning activity occurred.

POORLY COUPLED SUBDUCTION ZONES

Lesser Sunda Islands, Indonesia

Few thrust events of Mw≥5.5 and no known shocks of Mw≥7.7 occurred in Figure S1 along this subduction zone. One exception is where the continental margin of Australia is impinging on the subduction zone between 119^{o} and 120^{o} E where thrust shocks as large as Mw 6.5 occurred. Most earthquakes in the figure involved either strike-slip mechanisms along the inner wall of the subduction zone, thrust faulting along planes dipping to the south near the islands or normal faulting near the trench. This contrasts with the relatively greater numbers of thrust events shown earlier along well-coupled subduction interfaces. Normal-faulting shocks were relatively common near the trench including one in 1977 of Mw 8.3 (large open blue circle in Figure S1). It generated a large tsunami and was located far to the east of the two large Javanese earthquakes of 1994 and 2006 of in the main paper.

In summary, most of the Lesser Sunda islands were devoid of forerunning thrust activity just to the north of the trench. That part of the plate boundary appears to be poorly coupled as is that south of Java to the west. Many thrust events of moderate size occurred to the north of the island chain along faults that dip southerly. As Australia has converged with the Indonesian subduction zone, plate motion has jumped to the north side of the Sunda islands.

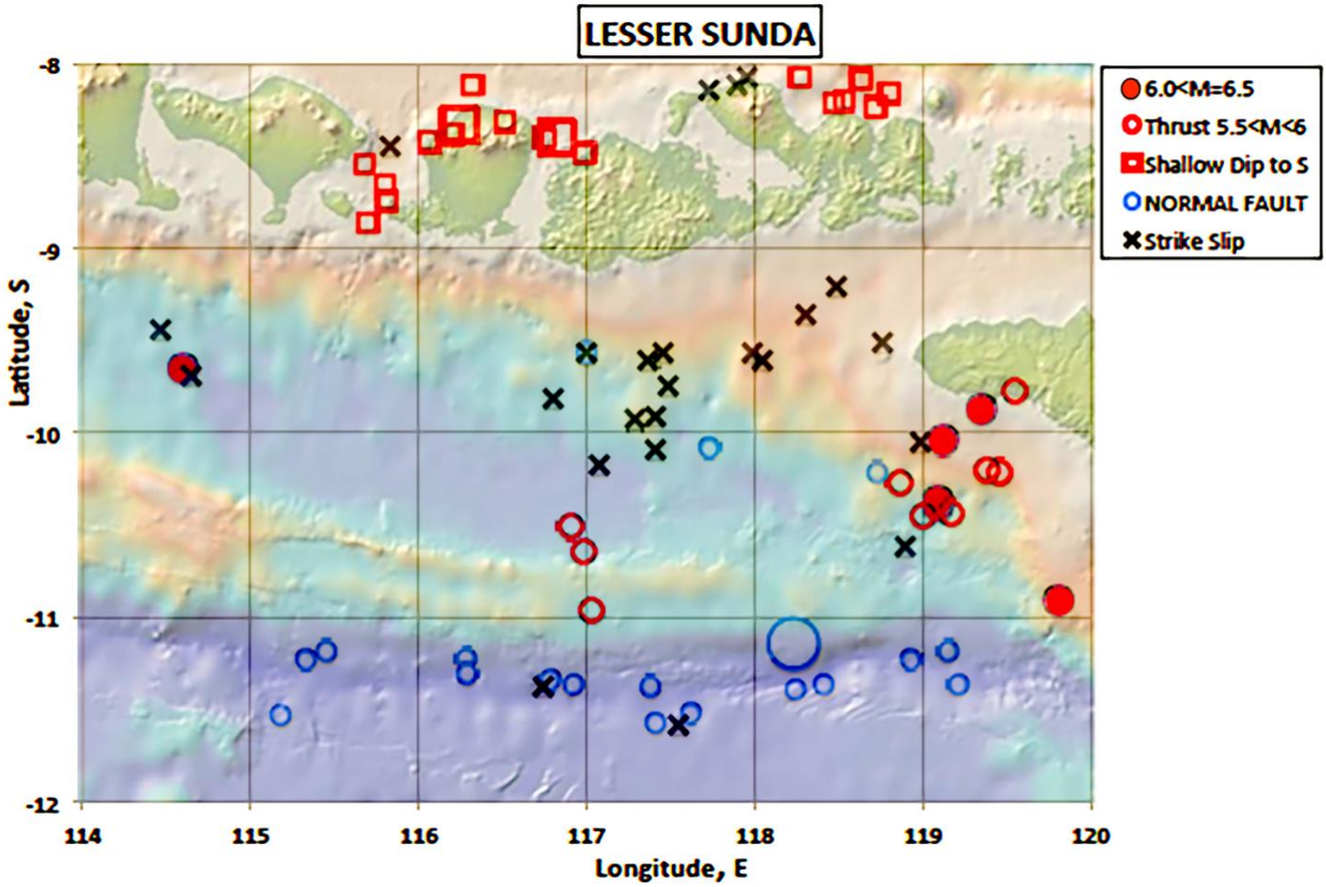

Figure S1. Locations of earthquakes near the Lesser Sunda Islands of Indonesia of Mw≥5.5 from 1977 through February 2019. Colors depict sizes and mechanisms of earthquakes.

Mariana Islands, Thrust Earthquake of 1993 near Guam, Mw 7.7

This was one of the smaller earthquakes examined. The Mariana subduction zone and its extension farther north along the Volcano, Izu and Bonin island arc are considered by most geoscientists to be poorly coupled. Seafloor (back arc) spreading occurs behind the subduction zone. Only two shocks in the Marianas of Mw>7.0 are known between 1976 and 2018 and one between 1916 and 1976. The subduction zone farther north has a similar paucity of events of those magnitudes except at its northernmost end near the Izu Peninsula of Japan. The Marianas have experienced a number of shocks of Mw<6.0 (not shown).

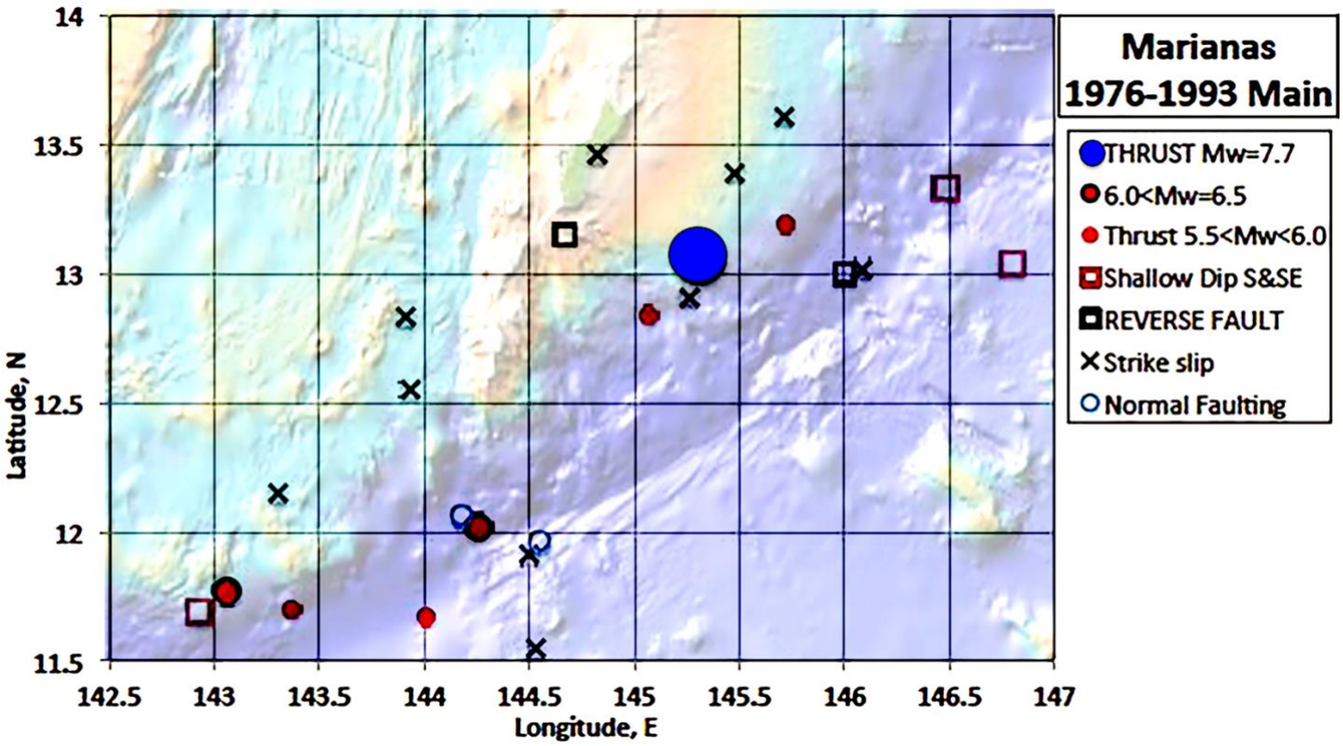

Figure S2. Earthquakes in the southern Mariana Islands of Mw≥5.5 from 1976 until the mainshock of 1993 (large blue circle). Colors denote sizes and mechanisms of earthquakes.

The largest known shallow earthquake (Mw 7.7) in the southern Marianas occurred in 1993. Harada and Ishibashi (2008) concluded it was an intraplate thrust event at a depth of 74 km in the downgoing Pacific plate, not an earthquake along the plate interface. Forerunning shocks of Mw≥5.5 between 1976 and its occurrence in 1993 were very few and most had strike-slip mechanisms (Fig. S2). Only two possible forerunning thrust events, each of Mw 5.5, took place within 150 km of the 1993 mainshock. A pattern of forerunning activity cannot be identified unless strike-slip mechanisms are included. The data reinforce the idea that the Mariana subduction zone is either mostly or entirely decoupled. To my knowledge a finite-fault computation has not been published.

In summary, the great thrust earthquake of 1993 appears to have occurred within the downgoing plate, not along the plate interface. Most, if not all, of the subduction zone along the southern Marianas is poorly coupled

An Unusual Thrust-Faulting Earthquake beneath Tonga in 2006, Mw 8.0

The Tonga-Kermadec plate boundary also is taken by most geoscientists to be poorly coupled. While thrust earthquakes as large as Mw 6.5 have occurred historically, few great thrust events are known. The number of earthquakes along the entire Tonga arc falls off rapidly as Mw increases (Figure S3). That activity

also drops off dramatically with depth (not shown). This supports the hypothesis of poor coupling for most of the shallow plate boundary. A number of asperities likely exist that are large enough to break in events of Mw<6.5.

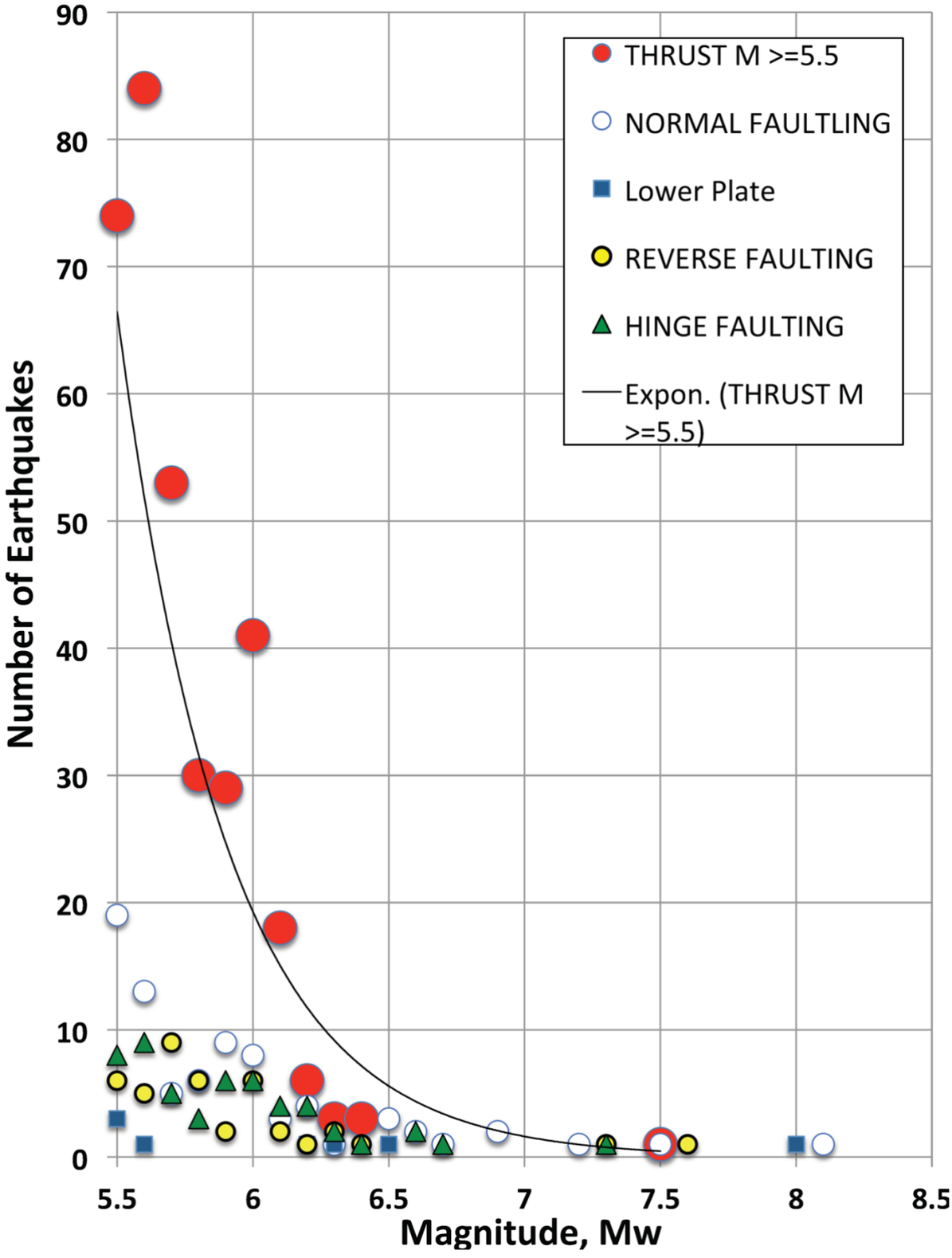

Figure S3. Number of Tongan earthquakes per 0.1 unit of magnitude Mw from 1977 through 2018.

Most thrust events in the centroid catalog are confined to the upper 20 km, which makes the thrust-faulting mainshock of 2006 unusual since its reported long-period (centroid) depth was 69 km. Meng *et al.* (2015) reanalyzed long-period P and surface waves and concluded the mainshock occurred at a similar depth. They analyzed data from regional seismic stations in Tonga and several GPS-observation points along the island chain. They deployed additional local stations after the mainshock. They concluded that the 2006 mainshock occurred within the downgoing Pacific plate 30 to 40 km below the plate boundary. Many of its aftershocks, however, were located above it close to the plate boundary. Their analysis of an Mw 7.6 earthquake farther south in Tonga near 23^{O} S in 2009 indicates it too occurred within the downgoing plate. Its mechanism, unlike that for the 2006 event, involved reverse faulting with a steeper dip.

Meng *et al*. performed a joint inversion of the slip distribution for the 2006 event. Since their computed zone of high slip extended outward only about 25 km, it was too small to compare it with locations of possible forerunning activity. Many long-period GCMT locations for thrust events appear to be biased at least 25 km to the east since they fall beyond the deepest part of the trench. The centroid location of the 2006 mainshock was located beneath the plate boundary but only 25 km from the deepest part of the trench. Those GCMT locations were likely biased too far east since they did not take into account sufficiently the spreading center of very of low velocity to the west of the Tongan arc in the Lau basin.

In summary, the 2006 earthquake ruptured within the downgoing Pacific plate at a depth of about 65 km and not along the plate boundary. It may have been like the great Kuril shock of 1994 described in the main body of the paper.

The Kermadec subduction zone extends from the southern end of the Tongan arc at 26^{O} S to northern New Zealand near 36^{O} S. Its largest thrust earthquake from 1976 through 2018 was of Mw 7.9. The three largest events from 1916 to 1976 were of Mw 7.8 to 8.1 (Pacheco and Sykes, 1992). Shallow shocks of Mw>7.0 since 1976 all occurred along just a part of the plate boundary between 28.7^{O} and 30.6^{O} S. Since most of them took place soon after the start of the GCMT catalog in 1976, forerunning activity could not be calculated for them using that catalog.

WELL-COUPLED SUBDUCTION ZONES WITH COMPLICATED OR POORER DATA

Jalisco, Mexico 1995, Mw 8.0

The 1995 mainshock of Mw 8.0 occurred along the Mexican subduction zone near a plate triple junction. The Cocos plate and the small Rivera plate underthrust the North American plate along the rupture zone of the 1995 earthquake. Only two forerunning events and a number of aftershocks with thrust mechanisms can be seen in Figure S4. Strike-slip activity, most of it after the mainshock, occurred just to the southwest along the Revilla Gigedo transform fault system.

In summary, the near lack of forerunning thrust activity is difficult to compare with the zones of high computed slip for this region of tectonic complexity.

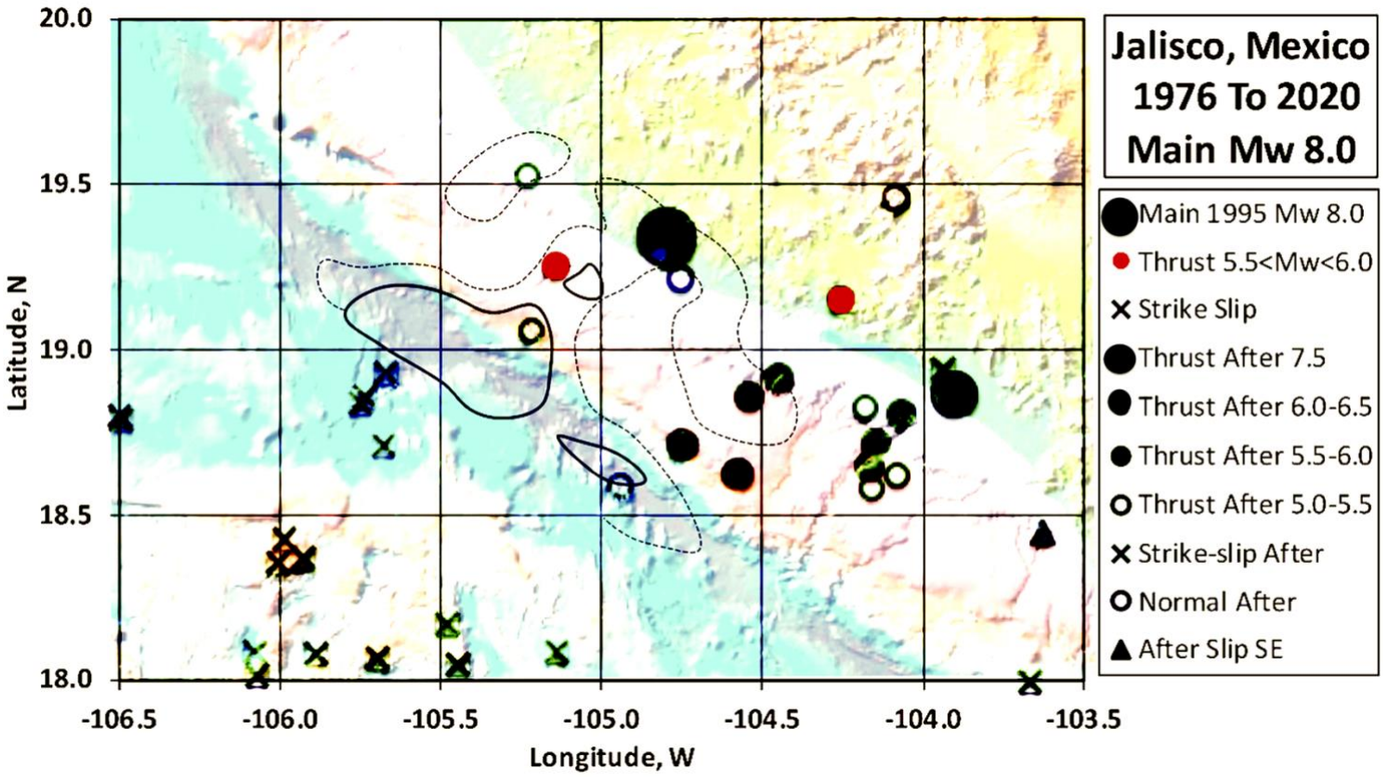

Figure S4. Locations of earthquakes off Jalisco, Mexico of Mw≥5.0 from 1976 through the mainshock of 1995 of Mw 8.0 (large black circle). Heavy and dashed lines indicate computed displacements of 2 and 1 m (from Mendoza and Hartzell, 1999).

Minahassa Peninsula of Sulawesi Island Earthquake of 1996, Mw 7.9

The 1996 mainshock of Mw 7.9 occurred along the northern peninsula of the Indonesian island of Sulawesi. The rocks of the peninsula consist of a major ophiolite complex. The thrust-fault mechanism of the mainshock and those of its aftershocks were situated at the western end of a subduction zone to the north and northwest of the peninsula. Its westernmost end abuts a major transform fault that strikes southerly. Gomez *et al.* (2000) found that the mainshock consisted of a simple pulse.

In summary, the centroid of the mainshock is situated inside the estimated high-slip area. That area is identified as a major asperity that broke in the mainshock. It was located at the intersection of thrust and

transform plate boundaries. Most forerunning activity was located more than 50 km from the small high-slip area.

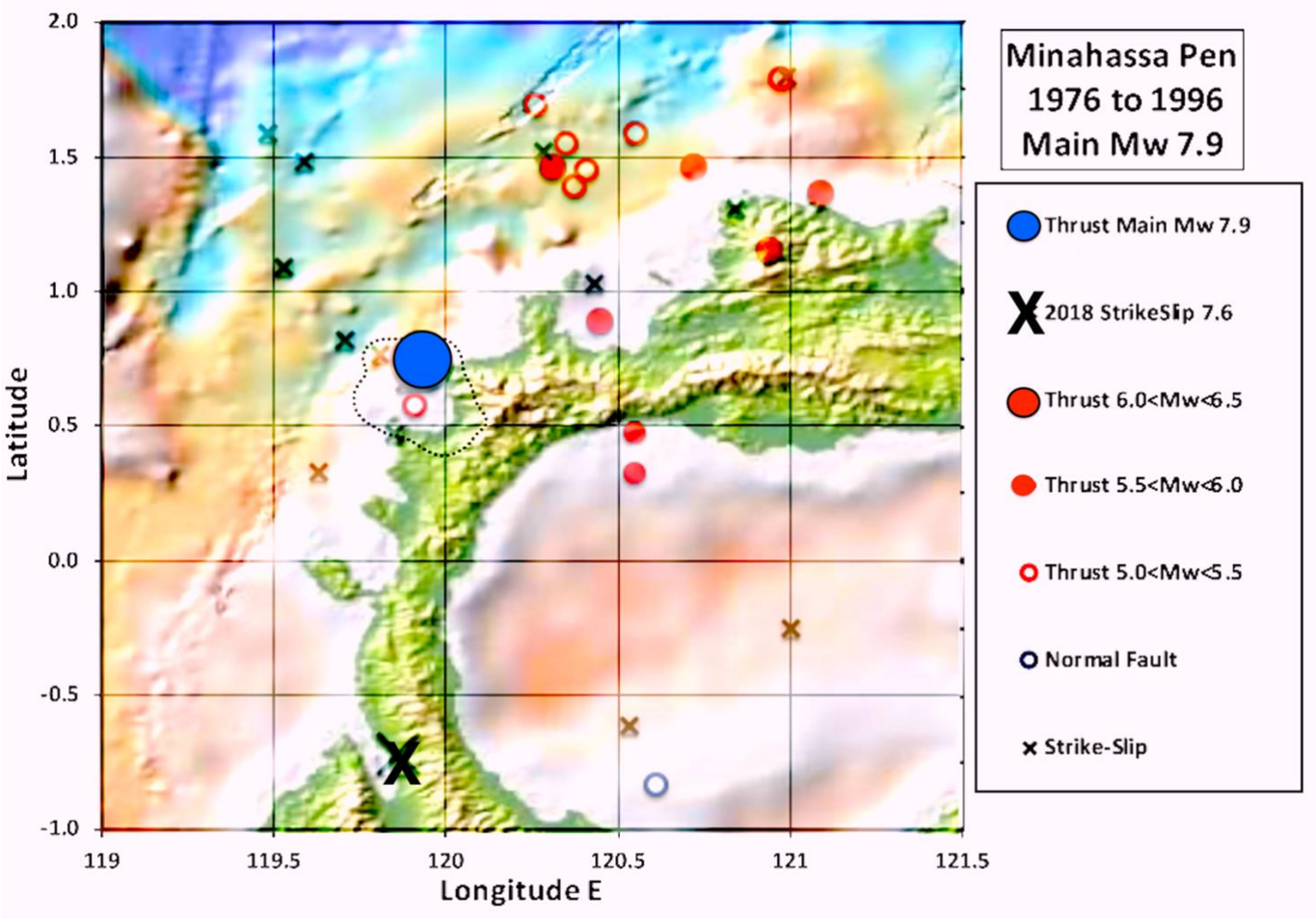

Figure S5. Locations of earthquakes of Mw>5.0 from 1976 until mainshock of 1996 of Mw 7.9 near the Minahassa Peninsula of Sulawesi, Indonesia. Large blue circle denotes centroid of mainshock. Dotted line encloses 85% of the area of computed slip (from Wetzler *et al*., 2018).

Irian Jaya, Indonesian Earthquake of 2009, Mw 7.7

The 2009 Irian Jaya shock of Mw 7.66 was one of the smallest earthquakes examined. It occurred near the northwest coast of New Guinea along the Manokwari trench, The computed slip contour in Figure S6 of 3 m, about half of the maximum, is quite small. A single shock of Mw 5 can be seen within that contour. The 1 m contour (not shown) extended about as far west as the aftershocks shown in the figure and about as far east as the large aftershock of Mw 7.4. Poiata *et al*. (2010) deduced that the mainshock consisted of a relatively simple source pulse.

In summary, the 3-meter slip contour, which extended about 40 km along strike, may define a relatively small asperity that ruptured in the mainshock. The numbers of forerunning shocks was small; uncertainties in their locations may well be sizable with respect to the size of the 3 m slip contour.

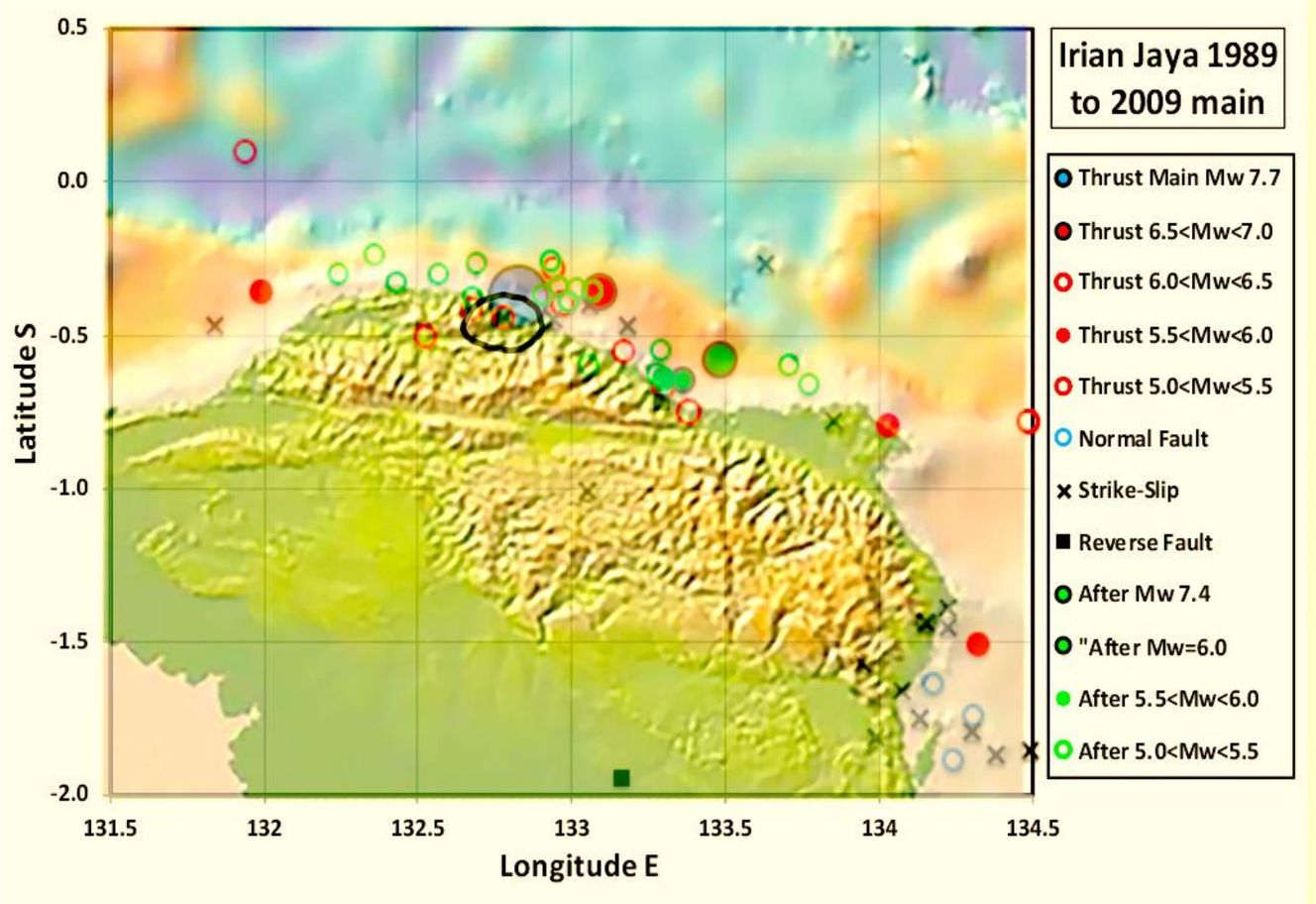

Figure S6. Locations of earthquakes near Irian Jaya, Indonesia of Mw>5.0 from 1989 until mainshock of Mw 7.7 of 2009. Large blue circle denotes centroid of mainshock. Black oval encloses computed displacement of 3 m and larger than from Poiata *et al*. (2010).

Triple Junction near New Ireland, New Britain and Bouganville—Papua New Guinea—Three Great Earthquakes of 2000, Mw 7.8 and 8.0

An unusual sequence of three great earthquakes occurred in and near New Ireland within 40 hours in 2000. The first of Mw 8.0, a strike-slip event (blue X in Fig. S7), ruptured the Weitin-Kamdaru fault, which crosses New Ireland with a strike of NNW (Tregoning *et* al., 2005). The two shocks of Mw 7.8 (large blue circles) were thrust events along the shallow-dipping, NNE-striking New Britain subduction zone. A major plate triple junction is present just to the south of the more eastern Mw 7.8 shock. The strike-slip event broke the surface of the Weitin-Kamdaru fault about 15 km far west its computed centroid. The fault then broke farther to the northwest in 2019.

Park and Mori (2007) modelled displacements during the Mw 8.0 event. They concluded that left-lateral, strike-slip motion first occurred within the island of New Ireland transitioning to a thrust component farther southeast. This helps to understand why the overall centroid mechanism indicated slip on a fault dipping 43^{O} NE. Park and Mori obtained a steeper dip and a larger Mw of 8.2. They find it ruptured as far southeast as the first Mw 7.8 shock.

I show estimated displacements by Park and Mori (2007) for the two largest thrust events, which are relatively small. They obtained Mw 7.5 and 7.4, smaller than the two GCMT values of 7.8. The centroids of the latter are located outside the maximum slip zones of Park and Mori. Forerunning thrust activity surrounds the centroid of the eastern thrust event of Mw 7.8. Only one thrust foreshock occurred within the 3 m slip zone, suggesting that mainshock may have occurred within a major asperity. Many forerunning thrust shocks occurred, however, within the 1 m slip zone of the second Mw 7.8 event. Its centroid lies outside that calculated slip zone.

In summary, the two largest thrust events of 2000 occurred in a complex three-plate tectonic setting. It is difficult to reconcile the locations of forerunning activity with the small size of their calculated zones of maximum slip. The latter do not agree with the two centroids, suggesting one of them is incorrect. Uncertainties in the locations of the centroids of thrust events of Mw 5.5 to 7.5 may be comparable to the sizes of the slip zones of the two largest thrust earthquakes.

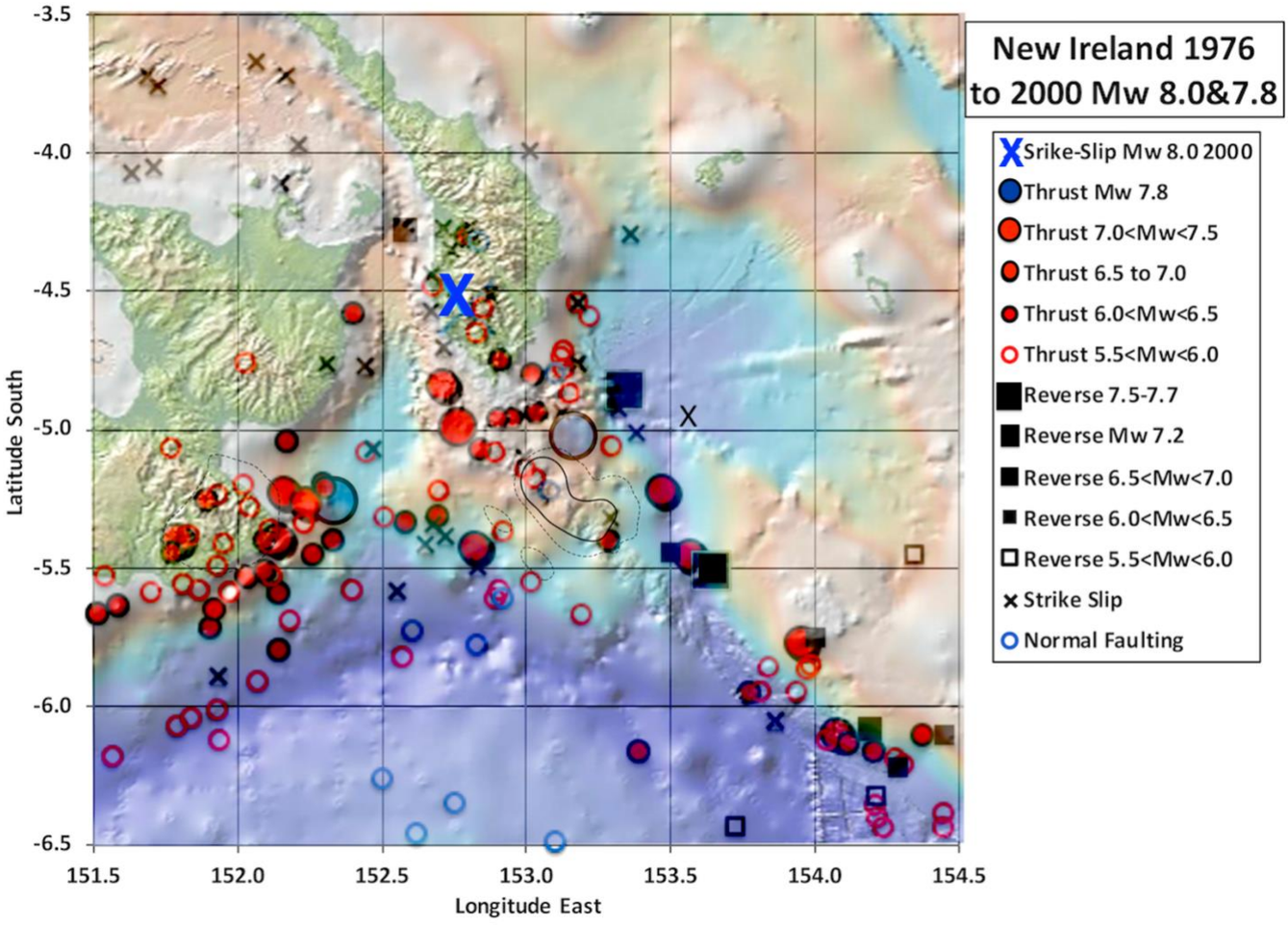

Figure S7. Locations of earthquakes near the plate triple junction south of New Ireland and east of New Britain. The first of three mainshocks on November 16 and 17 of Mw 8.0 involved strike slip faulting (large blue **X**). The next two mechanisms were thrust faulting of Mw 7.8 (two large blue circles). Computed displacements during the two thrust events of Mw 7.8 of 3 and 1 m are shown in solid and small dashed black lines (from Park and Mori, 2007).

New Ireland-Bouganville Earthquake of 2016, Mw 7.9

The 2016 shock along the Solomon subduction zone occurred about halfway between New Ireland and Bougainville island and to the southeast of the three great earthquakes of 2000 (Fig. S8). It was a reverse-faulting mechanism with a centroid depth of 53 km. Initial slip, however, began about 100 km to the north-north west at a depth of about 105 km (*Bulletin of International Seismological Centre*). Lay *et al*. (2016) modelled the initial 30 s of rupture as occurring over depths of 90 to 120 km on a fault dipping to the southwest. They conclude It was then followed by 50 s of rupture along the plate interface from depths of 32 to 47 km. Their calculated slip contours for the shallower half of their solution, solid and black lines in Figure S8, are situated well to the east of the centroid. They place deeper slip (not shown in Fig. S8) as extending farther north than that shallower.

In summary, the contours of maximum slip on the plate boundary by Lay *et al*. are located well to the east of the centroid of the mainshock. What asperities ruptured in the mainshock is uncertain.

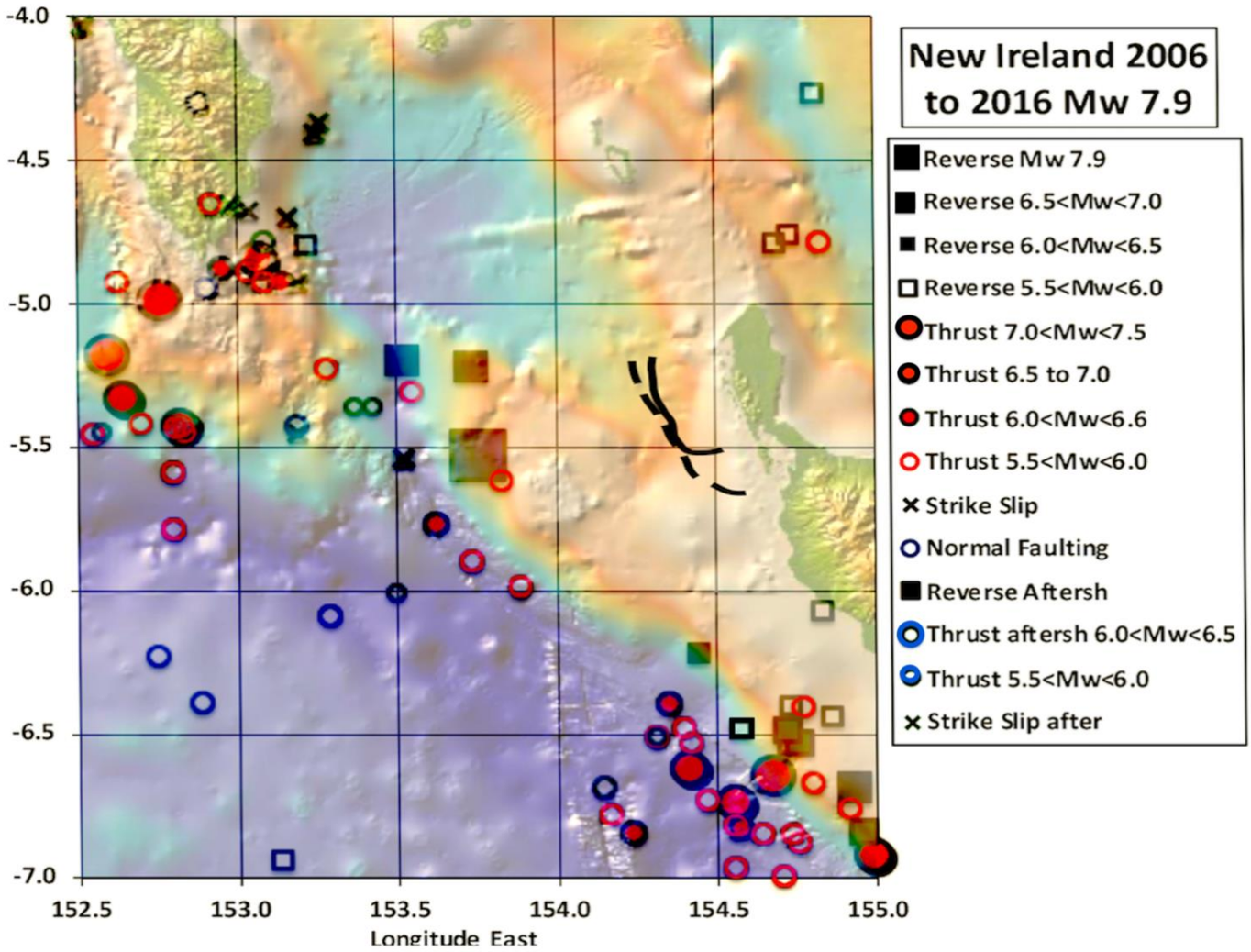

Figure S8. Locations of earthquakes of Mw≥5.5 south of New Ireland and west of Bougainville from 2006 until 2016 mainshock of Mw 7.9; aftershocks are also shown. Large black square indicates centroid of mainshock with its reverse-faulting mechanism. Black solid and dashed lines denote estimated maximum displacements of 2 and 1 m (from Lay *et al*., (2016).

Santa Cruz Earthquakes 2009, Mw 7.6 and 7.8

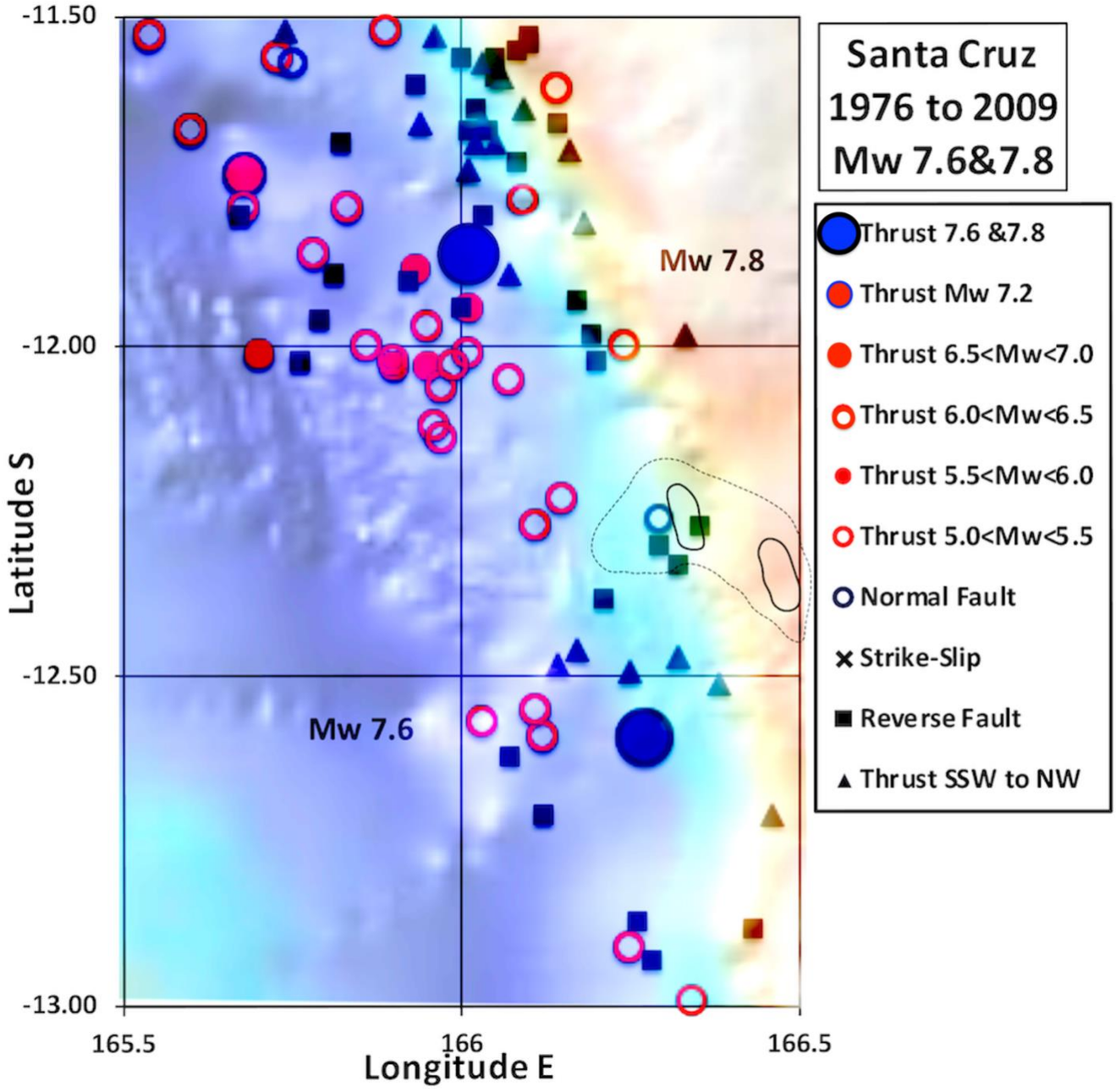

Figure S9. Locations of earthquakes in the Santa Cruz Islands of the southwest Pacific of Mw≥5.0 from 1976 through two 2009 mainshocks of Mw 7.6 and 7.8 (large blue circles). The Mw 7.8 shock occurred 15 minutes after the Mw 7.6. Hence, detailed slip in the Mw 7.8 could not be modelled. Solid and dashed lines denote estimated slip contours of 4 and 1.5 m (after Hayes, 2009) for the Mw 7.6 shock, one of the smallest mainshocks examined.

In summary, the calculated slip contours are about 35 km from the centroid of the 7.6 mainshock, making it difficult to determine the location of an asperity that ruptured during it. Thrust forerunning

activities surrounding both the Mw 7.6 and 7.8 centroids better define the two asperities broke in the mainshocks.

Vanuatu Earthquake of 1997, Mw 7.69

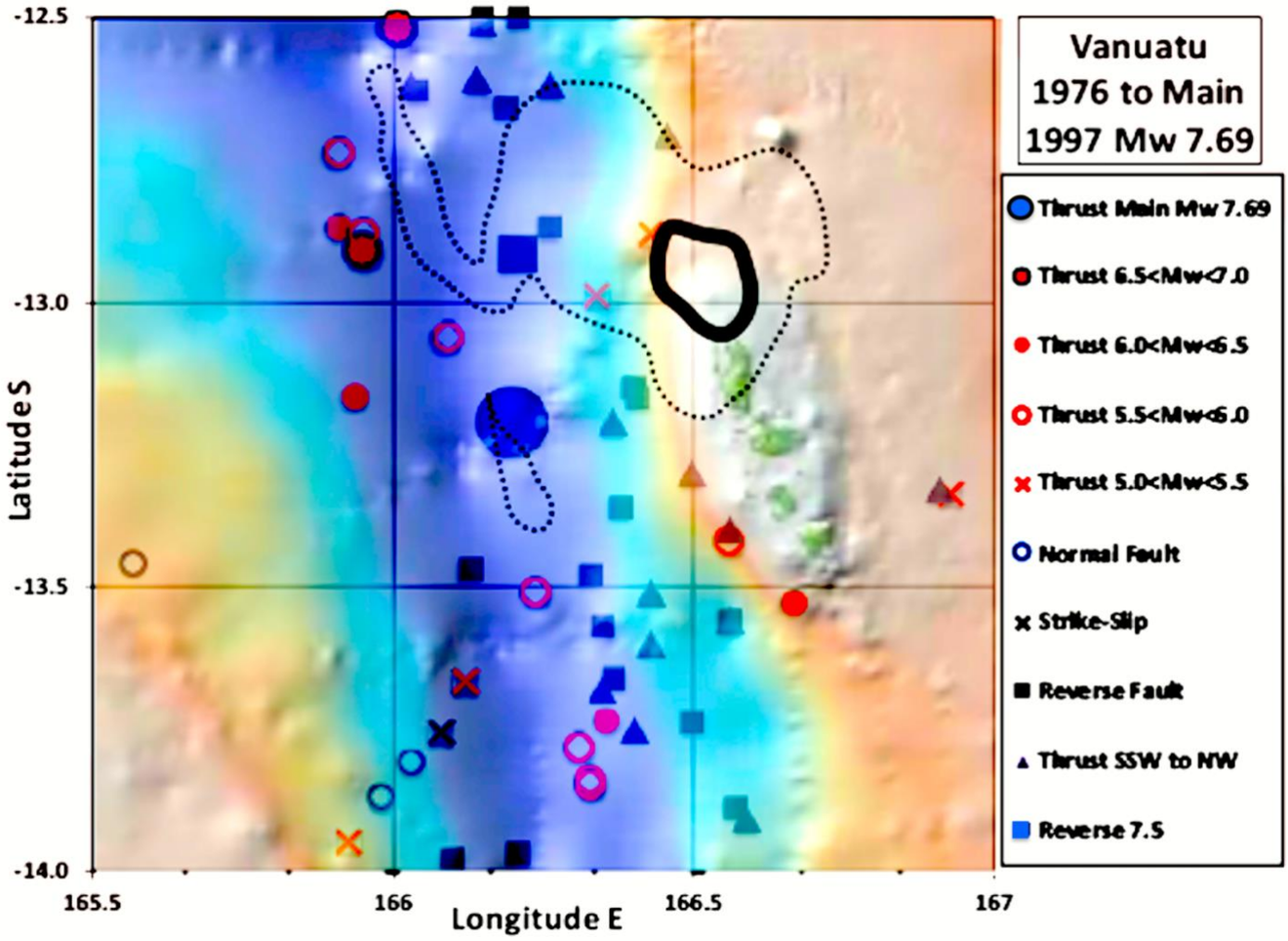

Figure S10. Locations of earthquakes in the Vanuatu islands of the southwest Pacific of Mw≥5.0 from 1976 through the 1997 mainshock of Mw 7.69 (large blue circle). Solid and dashed lines are contours enclosing 50 and 85% of the estimated slip areas in the mainshock (from Wetzler *et al.*, 2018).

The 1997 mainshock in the northernmost Vanuatu islands of Mw 7.69 was among the smallest earthquakes examined. Its centroid is situated along the inner wall of the Vanuatu (New Hebrides) trench (Fig. S10). It caused a moderate-sized tsunami (Kaverina et al., 1998). No forerunning activity occurred within the 50% slip contour. Most forerunning thrust and reverse activity was situated more than 25 km from the centroid. The centroid of the mainshock is located trenchward than most of the calculated high slip.

In summary, forerunning seismic activity was situated on three sides of the centroid of the mainshock and what is taken as a large asperity about 50 km along strike that ruptured in the mainshock. The centroid, however, is located seaward (trenchward) of the estimated large slip contours.

North Honshu Offshore Earthquake of 1994, Mw 7.73

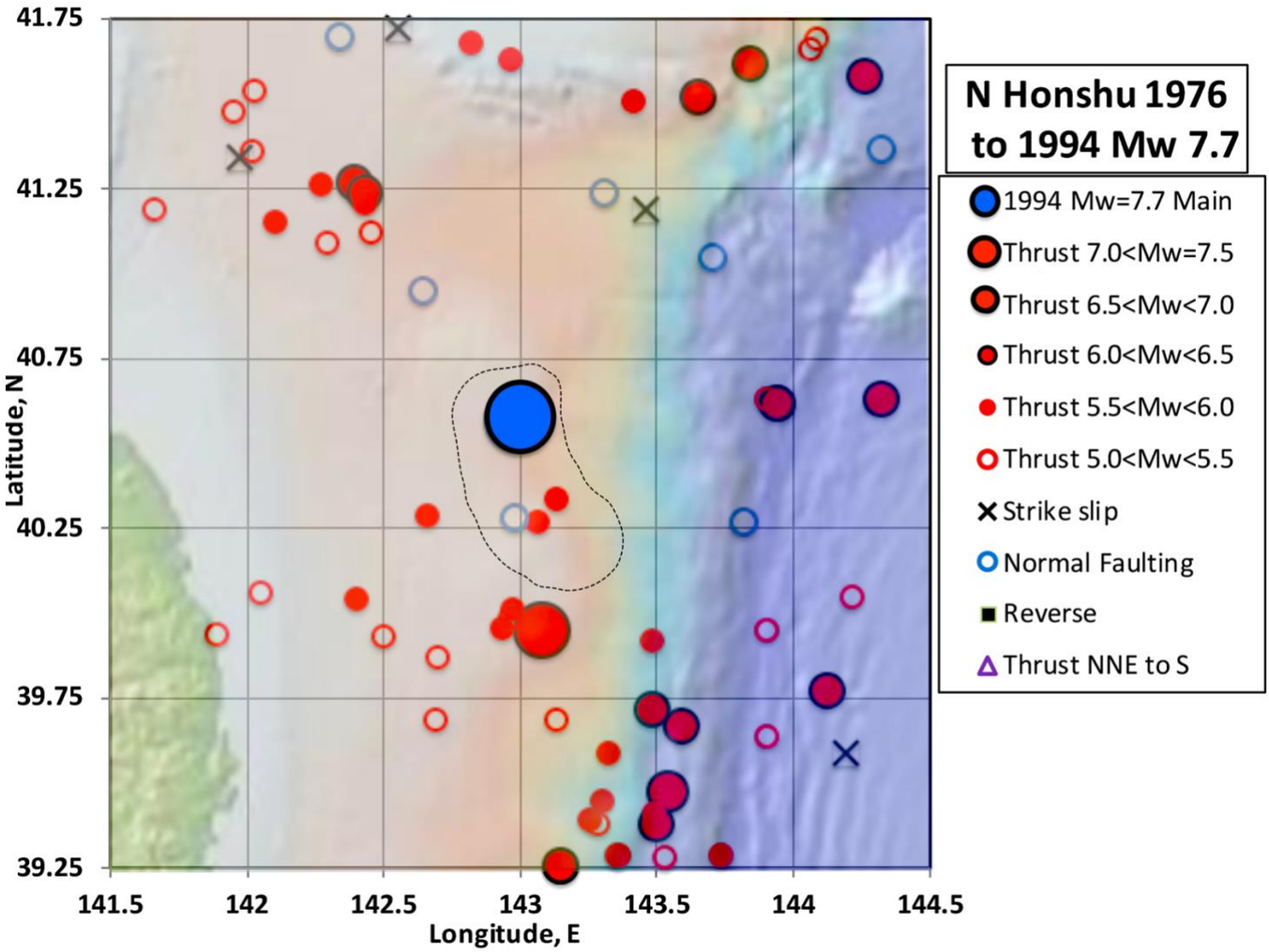

Figure S11. Earthquakes of M>5.0 from 1976 until the mainshock of 1994 (large blue circle) off the coast of northern Honshu, Japan of Mw 7.7. Dotted line encloses area of calculated displacement greater than 0.5 m (from Yagi *et al*., 2003).

The 1994 earthquake of Mw 7.73 occurred off the east coast of Honshu, Japan between the rupture zones of the great 1968 shock to the north and the giant 2011 Tohoku event to the south. The 1994 event was one of the smaller earthquakes studied; its maximum slip zone of (only 0.5 m in Fig. S11) extended about 75 km along strike and 35 km down dip. Possible uncertainties in the locations of nearby forerunning events may be a non-negligible fraction of those dimensions. Most forerunning activity occurred farther along strike

of the plate boundary and the centroid. Aftershocks through 1998 (not shown) took place largely outside the 0.5 m slip contour.

In summary, the 0.5 m slip contour contains the centroid of the mainshock. The large asperity that broke in the mainshock was surrounded by decadal forerunning activity. It includes the centroid and may extend somewhat farther northwest than the calculated slip contour.

Earthquake off the West Coast of Hokkaido Japan in 1993, Mw 7.7

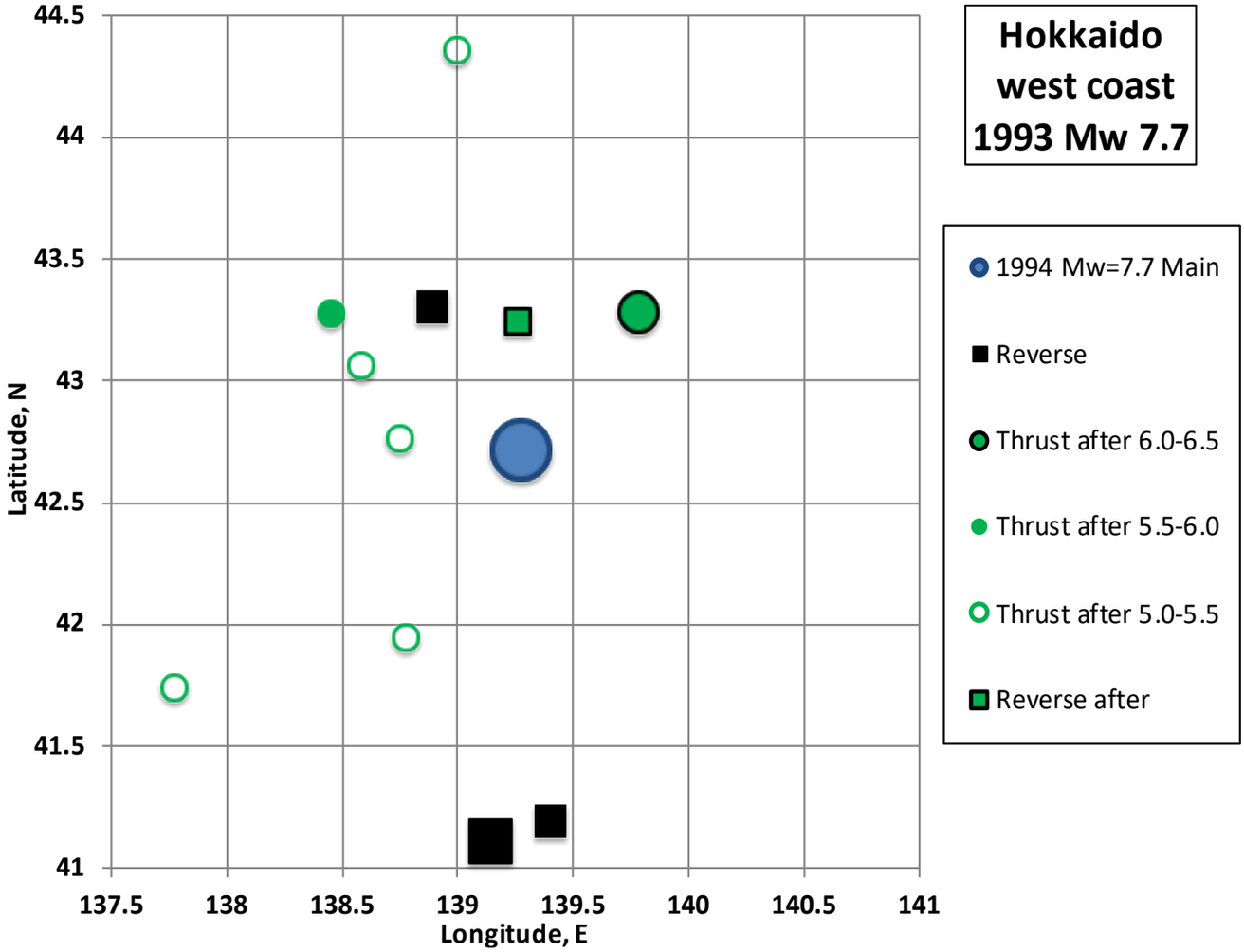

Figure S12. Forerunning activity from 1976 until mainshock off west coast of Hokkaido, Japan of 1993 (large blue circle).

The 1993 Japanese earthquake was one of the smaller events examined. It occurred off the west coast of the northern island of Hokkaido along a plate boundary with a very slow rate of long-term slip, especially when compared to that for the east coast of Honshu. This slow rate likely accounts for the lack of forerunning thrust activity and only three forerunning reverse-thrusting events in the 18 years before the mainshock (Fig S12). Several aftershocks surrounded the centroid of the mainshock at distances of 30 to 75

km. Kato and Tsuji (1994) computed two areas of large displacements (not shown) from tsunami arrival times and some geodetic data that extended from 42.95^{o} N to the north of the centroid to 41.8^{o} N to its south.

In summary, the centroid of the mainshock was centered inside the region of maximum computed slip. Aftershocks and the few forerunning events occurred outside that region. The mainshock likely took place within a large, poorly defined asperity along a plate boundary characterized by slow long-term motion

Earthquake off the Eastern Shumagin Islands, Alaska in 2020, Mw 7.8

Forerunning activity to the Shumagin Islands mainshock (Fig. S13) was mainly distributed either southwest or about 80 km to the northeast of both the centroid of the mainshock and the estimated zone of slip larger than 1.2 m. The slip zone (Figs. S13 and S14) was relatively small. Rupture in the mainshock (small blue circle in Fig. S14) initiated about 50 km ENE of the centroid.

Aftershocks of Mw$\geq$5.0 as of October 2020 were few. Figure S14 shows epicenters of aftershocks for short-period magnitudes greater than 4.5. Most occurred on three sides of the centroid and none to the south closer to the deepest part of the Aleutian trench. The main event did not generate a significant tsunami.

The 2020 shock may be a repeat of the Mw 7.5 earthquake of 1917. The short-period location of the 1917 mainshock and four aftershocks as relocated by Boyd and Lerner-Lam (1988) form a band encircling the 2020 centroid (Fig. S14). A mainly strike-slip event of Mw 7.6 broke to the south of the computed rupture zone and centroid of the July mainshock on 19 October 2020.

In summary, the centroid of the 2020 Shumagin earthquake occurred in a relatively quiet zone surrounded by some forerunning activity and aftershocks. The zone of estimated slip larger than 1.2 m coincides with the quiet zone. It defines an asperity with dimensions of about 40 by 50 km. Approximately the same zone broke in 1917 but in a smaller mainshock. The section of the plate boundary to the northeast last broke in 1938 in a great thrust earthquake of Mw 8.1 (Pacheco and Sykes, 1992). The adjacent plate boundary to the southwest appears to be poorly coupled (Li and Freymueller, 2018) and did not rupture in July 2020.

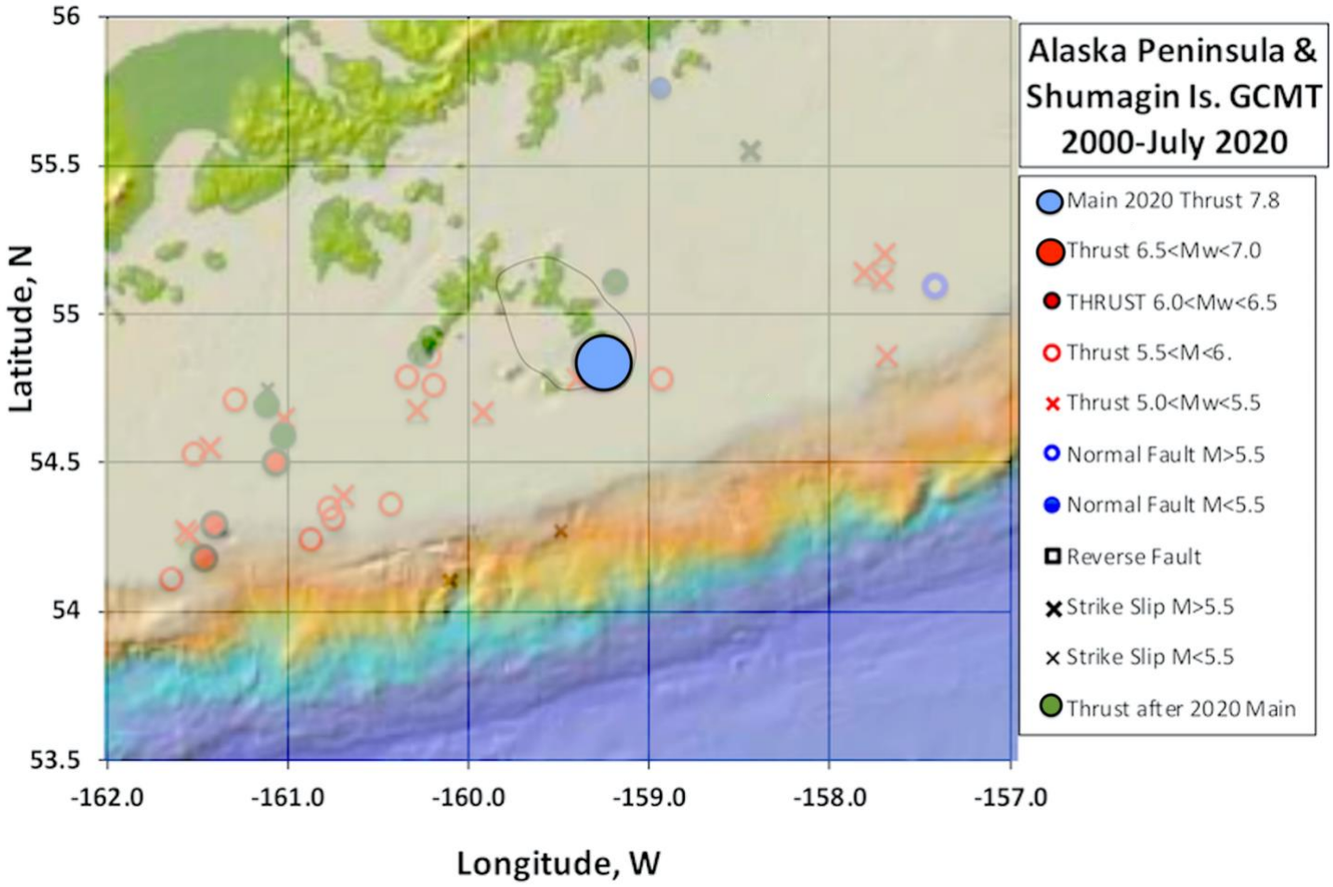

Figure S13. Forerunning events of Mw>5.0 from 2000 until Shumagin Islands earthquake of July 22, 2020. Large blue circle denotes mainshock. Aftershocks shown through 20 October 2020. Black oval denotes estimated zone of slip greater than 1.2 m during July mainshock (from Crowell and Melgar, 2020).

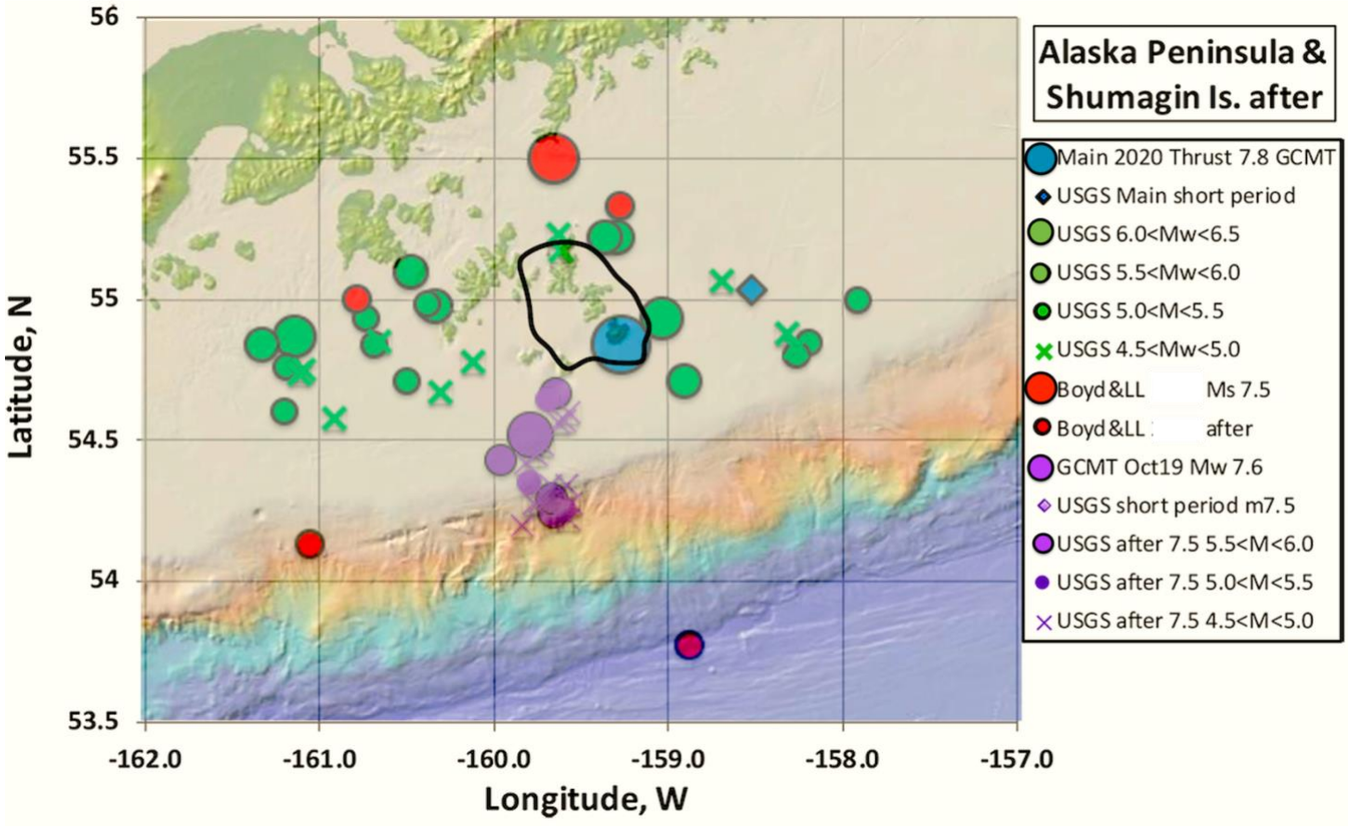

Figure S14. Aftershocks through 19 Oct 2020 for the Shumagin Islands earthquake of July 22, 2020 of short-period magnitudes greater than 4.5 as determined by the U.S. Geological Survey. Large blue circle denotes centroid of mainshock. Red circles denote short-period locations of mainshock of 1917 (largest circle) and its aftershocks from Boyd and Lerner-Lam (1988). Purple indicates mainshock of Mw 7.5 of 19 Oct 2020 and three days of aftershock activity. Slip contour same as in previous figure.

Flores Indonesia Earthquake of 1992, Mw 7.7

The earthquake of 1992 occurred along the Lesser Sunda region of Indonesia near the north side of Flores island (Fig. S15). It is one of the smallest mainshocks studied. Its mechanism involved thrust faulting with a southerly dip, like events just to its west in Figure S1. In those two areas Australia has converged with Indonesia with much plate motion now occurring on the north side of the former north-dipping subduction zone. Pranantyo and Cummins (2019), who state that more than 3000 lives were lost in the destructive earthquake and its large tsunami, describe the tectonics in greater detail.

The zones of high computed slip were devoid of forerunning activity in Figure S15 as well as aftershocks (not shown). The two largest are interpreted as major asperities.

In summary, the zones of high computed slip were devoid of forerunning activity. They are interpreted as major asperities.

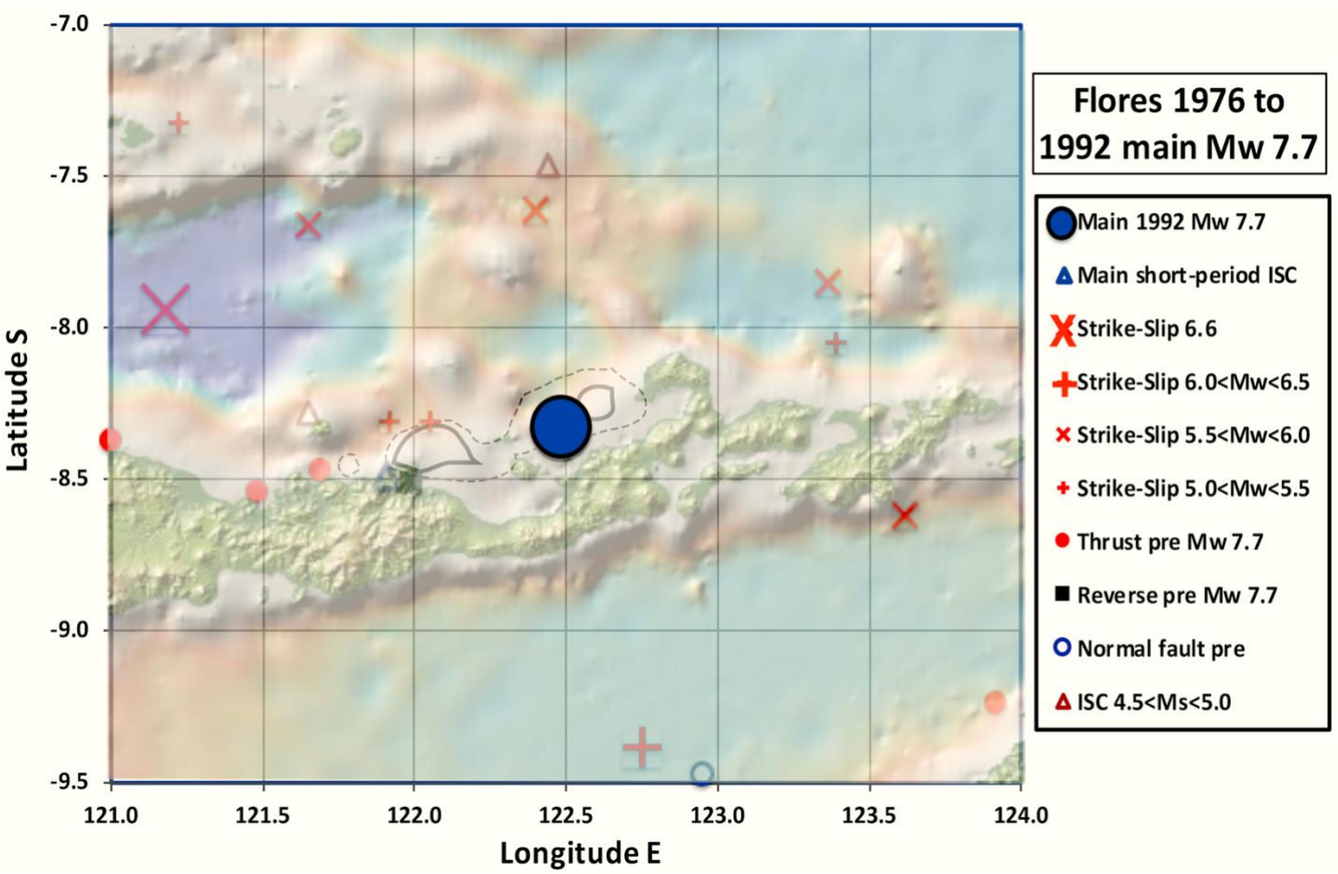

Figure S15. Flores Indonesian mainshock of 1992, Mw 7.7 (large blue circle). Solid and dashed contours denote computed slip greater than 10 and 4 m (from Pranantyo and Cummins, 2019).

Nepal Earthquake of 2015, Mw 7.9

The Nepal shock of 2015 occurred along a continental convergence plate boundary, not a subduction zone. It is included here because of the similarity of its thrust mechanism to those at subduction zones. Not enough forerunning activity took place (Fig. S16), however, for it to be compared with details of the computed slip in the mainshock.

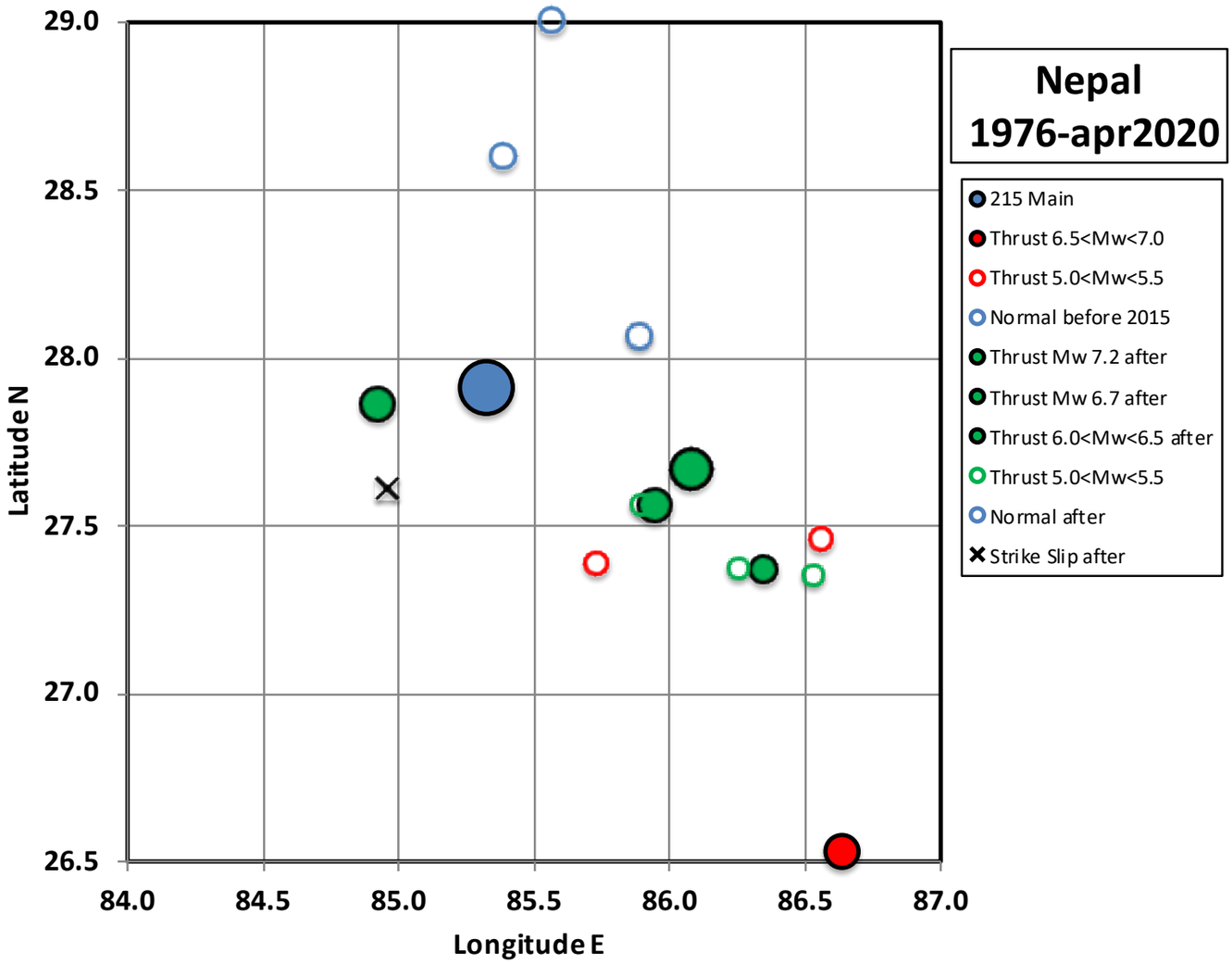

Figure S16. Forerunning and aftershock activity for Nepal earthquake of 2015. Large blue circle denotes centroid of mainshock.

Haida Gwaii (Queen Charlotte) Canada **thrust earthquake of 2012, Mw 7.8**

The 2012 mainshock was unusual in that it was a great thrust event just to the west of the Queen Charlotte strike-slip fault. That plate boundary is largely a transform fault but one with a smaller thrust component. Only one thrust foreshock (Fig. S17) occurred between 1976 and the mainshock. All but one of the aftershocks shown involved normal faulting. Lay *et al.* (2013) found that slip in the mainshock (not shown) was concentrated largely between the coastline and the normal-fault aftershocks within the hard-rock of the upper plate beneath a young sedimentary basin.

In summary, the mainshock is not explored further since the number of forerunning earthquakes was so small. It was an unusual thrust earthquake that occurred adjacent to the main strike-slip fault of the plate boundary that last ruptured in a great strike-slip mainshock in 1949.

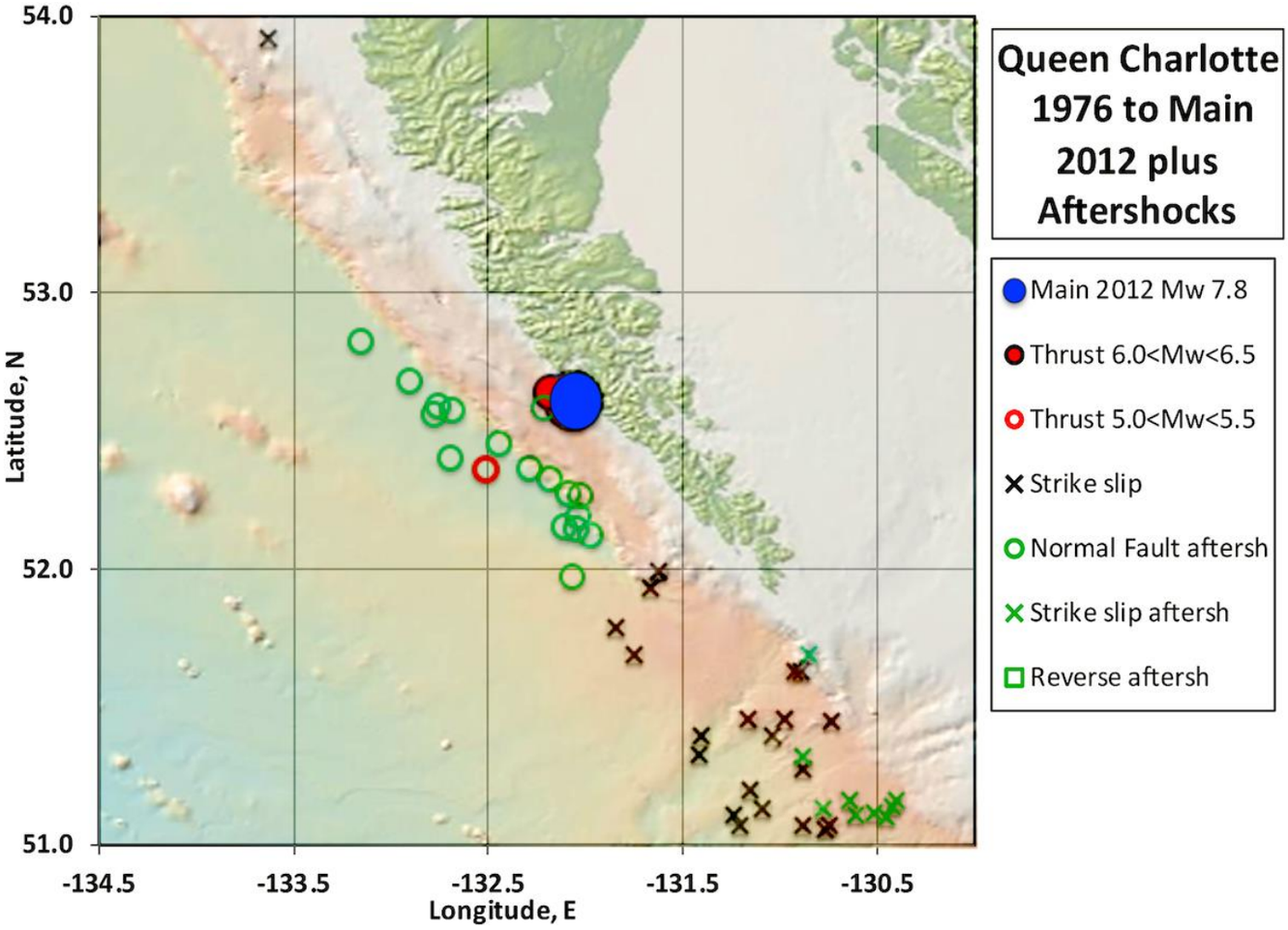

Figure S17. Forerunning and aftershock activity to the Haida Gwaii (Queen Charlotte) earthquake of 2012. Large blue circle denotes centroid of mainshock.

ADDITIONAL REFERENCES FOR SUPPLEMENTARY SECTION

Boyd, T. M., and A. L. Lerner Lam (1988). Spatial distribution of turn-of-the-century seismicity along the Alaska-Aleutian arc, *Bull. Seismol. Soc. Amer*. **78**, 636-650.

Crowell, B. W. and D. Melgar (2020). Slipping the Shumagin gap: a kinematic and early afterslip model of the Mw 7.8 Simeonof Island, Alaska, earthquake, *Geophys. Res. Lett.* **47** (19), **https://doi.org/10.1029/2020GL090308**

Gomez, J. M., R. Madariaga, A. Walpersdorf and E. Chalard (2000). The 1996 earthquake in Sulawesi, Indonesia, *Bull. Seismol. Soc. Amer*. **90**, 739-751.

Hayes, G. P. (2009). M7.6, 7.8 and 7.3 Vanuatu region earthquakes of 7 October 2009. U.S. Geological Survey, unpublished document, 1 page.

Kato, K., and Y. Tsuji (1994). Estimation of fault parameters of the 1993 Hokkaido-Nansei-Oki earthquake and tsunami characteristics, *Bull. Earthquake Res. Inst. Tokyo Univ*., 69, 39-66.

Kaverina, A., D. Dreger, and M. Antolik (1998). Source process of the 21 April 1997 Santa Cruz Island earthquake (Mw 7.8), *Geophys. Res. Lett*. **25**, 4027-4030.

Lay, T., L. Ye, H. Kanamori, Y. Yamazaki, K. F. Cheung, K. Kwong, and K. D. Koper (2013). The October 28, 2012 Mw 7.8 Haida Gwaii underthrusting earthquake and tsunami: slip partitioning along the Queen Charlotte fault transpressional plate boundary, *Earth Planetary Science Letters* **375**, 57-70.

Lay, T., L. Ye, C.J. Ammon, and H. Kanamori (2016). Intraslab rupture triggering megathrust rupture Coseismically in the 17 December 2016 Solomon Islands Mw 7.9 earthquake, *Geophys. Res. Lett.* **44,** doi.org/10.1002/2017GL072539, 20 pp.

Li, S., and J. T. Freymueller (2018). Spatial variation of slip behavior beneath the Alaska Peninsula along Alaska-Aleutian subduction zone, *Geophys. Res. Lett*. **45**, 3453-3460.

Mendoza, C., and S. Hartzell (1999). Fault-slip distribution of the Colima-Jalisco, Mexico, earthquake, *Bull. Seismol. Soc. Amer*. **109**, 1338-1344.

Meng, Q., D. S. Heeszel, L. Ye, T. Lay, D. A. Wiens, M. Jia, and P. R. Cummins (2015). The 3 May 2006 (Mw 8.0) and 19 March 2009 (Mw 7.6) Tonga earthquakes: intraslab compressional faulting below the megathrust, *J. Geophys. Res*. **120**, 6297-6316.

Park, S.-C., and J. Mori (2007). Triggering of earthquakes during the 2000 Papua New Guinea earthquake sequence, *J. Geophys. Res*. **112**, doi.org/10.1029/2006JB004480.

Poliata, N., K. Koketsu, and H. Miyake (2010). Source processes of the Irian Jaya, Indonesia, earthquake doublet, *Earth Planets and Space* **62**, 475-481.

Pranantyo, I. R., and P. R. Cummins (2019). Multi-data-type source estimation for the 1992 Flores earthquake and tsunami, *Pure Appl. Geophysics* **176**, 2969-2983.

Tregoning, P., M. Sambridge, H. McQueen, S. Toulmin, and T. Nicholson (2005). Tectonic interpretation of Aftershock relocations in eastern Papua New Guinea using teleseismic data and the arrival pattern method, *Geophys. J. Intern*. **160**, 1103-1111.

Yagi, Y., M. Kikuchi, and T. Nishimura (2003). Co-seismic slip, post-seismic slip, and largest aftershock associated with the 1994 Sanriku-haruka-oki, Japan earthquake, *Geophys. Res. Lett*. **30**, 2177, doi:10.1029/2003GL018189